HHS Public Access

Author manuscript

Mol Omics. Author manuscript; available in PMC 2023 August 15.

Published in final edited form as:

Mol Omics. ; 18(7): 627–634. doi:10.1039/d2mo00115b.

Rbm20 ablation is associated with changes in the expression of titin-interacting and metabolic proteins

Eli J. Larson[1,†], **Zachery R. Gregorich**[2,†], **Yanghai Zhang**[2], **Brad H. Li**[1], **Timothy J. Aballo**[1], **Jake A. Melby**[1], **Ying Ge**[1,3], **Wei Guo**[2,*]

[1]Department of Chemistry, University of Wisconsin-Madison, Madison, WI, USA

[2]Department of Animal and Dairy Sciences, University of Wisconsin-Madison, Madison, WI, USA

[3]Department of Cell and Regenerative Biology, University of Wisconsin-Madison, Madison, WI, USA

Abstract

Dilated cardiomyopathy (DCM) is a major risk factor for developing heart failure and is often associated with an increased risk for life-threatening arrhythmia. Although numerous causal genes for DCM have been identified, RNA binding motif 20 (Rbm20) remains one of the few splicing factors that, when mutated or genetically ablated, leads to the development of DCM. In this study we sought to identify changes in the cardiac proteome in Rbm20 knockout (KO) rat hearts using global quantitative proteomics to gain insight into the molecular mechanisms precipitating the development of DCM in these rats. Our analysis identified changes in titin interacting proteins involved in mechanical stretch-based signaling, as well as mitochondrial enzymes, which suggests that activation of pathological hypertrophy and altered mitochondrial metabolism and/or dysfunction, among other changes, contribute to the development of DCM in Rbm20 KO rats. Collectively, our findings provide the first report on changes in the cardiac proteome associated with genetic ablation of *Rbm20*.

Graphical Abstract

[*]To whom correspondence should be addressed: Dr. Wei Guo, 1933 Observatory Dr., Madison, WI 53706, United States. Tel.: +1 608-263-3676; wguo2@wisc.edu.
[†]Equal Contribution

Conflicts of interest
There are no conflicts of interest to declare.

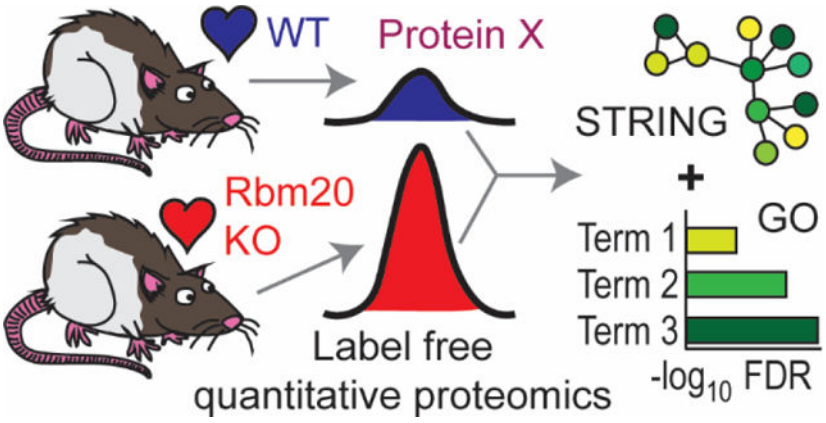

Label-free quantitative proteomics identifies molecular correlates of dilated cardiomyopathy in rats lacking the muscle-specific splicing factor Rbm20.

Keywords

Dilated Cardiomyopathy; Heart Failure; Rbm20; Titin; Mitochondrial Metabolism; Proteomics

Introduction

Dilated cardiomyopathy (DCM) is a non-ischemic heart muscle disease characterized by left or biventricular dilation and impaired systolic function in the absence of abnormal loading conditions or coronary artery disease.[1] DCM is estimated to affect approximately 1 in 250 individuals in the general population and remains a significant cause of worldwide morbidity and mortality despite advances in the management of heart failure in patients with DCM.[2] While mutations in the *TTN* gene, which encodes the giant sarcomeric protein titin, are the most common cause of DCM and account for approximately 20–25% of cases,[3] the genetics of DCM are complex with mutations in over 60 genes having been linked to this disease.[4] Among the myriad DCM-linked genes that have been identified, RNA binding motif 20 (Rbm20) is unique as it is one of only a handful of splicing factors that, when mutated or genetically ablated in humans and animal models, leads to the development of DCM.[5–8] Mutations in RBM20 are estimated to account for ~3% of familial cases of DCM.[9,10]

Rbm20 is a *trans*-acting splicing factor that is highly expressed in skeletal and cardiac muscle.[11] To date, Rbm20 has been shown to regulate the alternative splicing of more than 30 genes, the most well-studied of which is *TTN*.[11] Loss-of-function studies in Rbm20 knockout (KO) rats and mice demonstrated that Rbm20 not only modulates myocardial stiffness by regulating titin isoform expression, but also affects cardiomyocyte contractility via the splicing regulation of genes involved in calcium handling, such as *Ryr2* and *Camk2d*.[12,13] Indeed, the DCM-like phenotype that develops in Rbm20 KO rats and mice is thought to result primarily from 1) reduced diastolic stiffness due to the expression of more compliant titin isoforms and 2) impaired contractility secondary to alternative splicing of calcium handling genes.[11–14] Yet, the possibility that additional factors contribute to the development of DCM in Rbm20 KO animals cannot be ruled out.

In an effort to identify additional networks of dysregulated genes in Rbm20 KO rats that could contribute to the development of DCM, we previously employed global transcriptome profiling.[12] This approach enabled the identification of changes in the expression of approximately 400 genes, including titin-interacting and Ca^{2+}-handling genes, in the KO rat ventricular myocardium throughout post-natal development;[12] however, given the notoriously poor correlation between transcript and protein levels,[15–17] examination of gene expression at the protein level to identify genes with altered expression in Rbm20 KO animals is warranted. Thus, in this study, we employed global quantitative mass spectrometry (MS)-based proteomics to profile changes in the cardiac proteome in Rbm20 KO rats and gain insight into alterations precipitating Rbm20 deficiency-associated DCM at the protein level.

Materials and methods

Chemicals and reagents

All reagents were purchased from Millipore Sigma unless otherwise noted. HPLC grade water, formic acid, and acetonitrile were purchased from Fisher Scientific (Fair Lawn, NJ, USA). 4-Hexylphenylazosulfonate (Azo) was synthesized in-house as previously described.[18,19]

Animals and tissue collection

Male and female wild type (WT) and Rbm20 homozygous knockout (KO) rats (*Rattus norvegics*) were used in this study. Rbm20 KO rats have been described previously.[11,20] All rats were crosses of Sprague-Dawley (SD) × Brown Norway (BN) (all strains were originally obtained from Harlan Sprague Dawley, Indianapolis, IN, USA). Rats with mixed genetic background were backcrossed three generations with pure SD strain resulting in rats that have a genetic background that is approximately 96% SD and 4% BN. Animals were maintained on a standard rat chow diet. All procedures involving animals were carried out following the recommendations in the Guide for the Care and Use of Laboratory Animals published by the National Institutes of Health and were approved by the Institutional Animal Care and Use Committee of the University of Wisconsin-Madison. WT and KO rats (n = 8 each) were sacrificed at three weeks-of-age, hearts were excised, snap frozen in liquid nitrogen, and stored at −80 ºC for later use.

Protein extraction

Protein extracted from approximately 120 mg of ventricular tissue were prepared using the procedure developed by Aballo *et al.*[21] to fit the scale used by Jin *et al.*[22] Briefly, tissue was washed twice in 2 mL of Mg^{2+}/Ca^{2+}-free DPBS containing 1× HALT protease and phosphatase inhibitor cocktail (Thermo Fisher Scientific, Waltham, MA, USA). After washing, tissues were homogenized in 1.5 mL of lysis buffer (25 mM ammonium bicarbonate, 10 mM L-methionine, 1 mM dithiothreitol (DTT), and 1x HALT protease and phosphatase inhibitor cocktail) using a Pro 200 electronic homogenizer from Pro Scientific Inc. (Oxford, CT, USA). After initial homogenization, 1.5 mL of Azo[19] extraction buffer (0.2% w/v Azo, 25 mM ammonium bicarbonate, 10 mM L-methionine, 1 mM DTT, and 1x HALT protease inhibitor cocktail) was added and samples were homogenized a second

time. Homogenates were centrifuged at 21,100 × *g* for 30 min (4 °C) and the supernatants were recovered. The recovered protein extracts were analyzed by SDS-PAGE to assess the reproducibility of protein extraction, digested for liquid chromatography (LC)-tandem MS (MS/MS), and used for Western blot analysis.

Protein digestion and LC- MS/MS analysis

The concentration of protein extracts was determined using the Bradford protein assay and 100 μg of total protein from each sample was digested using the one-hour digestion procedure employed by Aballo *et al.*[21] Resulting peptides were desalted using Pierce C18 Tips from Thermo Fisher (Waltham, MA, USA) following the manufacturer's instructions. Samples were evaporated to dryness under vacuum then reconstituted in mobile phase A (0.2% formic acid in water). The concentration of samples was determined using a NanoDrop One^{c} Microvolume UV-Vis Spectrophotometer from Thermo Fisher Scientific and all samples were adjusted to a final volume of 0.2 mg/mL with mobile phase A. Peptides were separated by reverse phase LC (RPLC) using a Bruker nanoElute with an IonOpticks Aurora CSI C18 column, injecting 1 μL and using a 90 minute stepped gradient of 5-5-65-95-100-5-5% mobile phase B (0.2% formic acid in acetonitrile) over 0-5-65-95-105-106-120 minutes at 55 °C. Detection of separated peptides was performed though online coupling with a Bruker timsTOF Pro using data-dependent analysis to select the top-10 precursor intensities and fragment by parallel accumulation serial fragmentation (PASEF).[23]

Western blot

Azo-containing protein extracts were mixed with 4× Laemmli buffer, boiled at 98 ^{o}C for 3 min, and resolved by SDS-PAGE on homemade 10% polyacrylamide gels. Proteins were transferred to Immun-Blot PVDF Membranes for Protein Blotting (0.2 μm pore size, Bio-Rad, cat# 1620177) at 300 mA for 90 min in a cold room (4 ^{o}C). To block, membranes were incubated in TBST with 5% (w/v) nonfat dry milk for 1 hr at room temperature, followed by incubation in primary antibody solution containing 5% (w/v) nonfat dry milk and diluted Msrb2 (1:500, Proteintech, cat# 17629-1-AP) or Gapdh (1:1000, Cell Signaling Technology, cat# 2118) primary antibodies in TBST overnight at 4 ^{o}C. The membranes were removed from primary antibody solution and washed 5 × 5 min with TBST followed by incubation in TBST with 3% (w/v) nonfat dry milk and diluted secondary antibody (1:3000, Promega, cat# W4018) for 1 hr at room temperature. Subsequently, membranes were washed 5 × 5 min with TBST, overlayed with SuperSignal West Pico PLUS Chemiluminescent Substrate (Thermo Fisher Scientific, cat# 34577), and imaged using a ChemiDoc Imaging System (Bio-Rad). Band densities were quantified using ImageJ.[24] Msrb2 band densities were first normalized to Gapdh and then to a replicate WT sample loaded on each gel yielding relative Msrb2 intensities normalized to Gapdh. The significance of the difference between group means was determined using a two-tailed Student's *t*-test.

Data analysis

Data analysis was performed using MaxQuant (v1.6.5.0) to search all reviewed canonical and isoform data for *Rattus norvegicus* in Uniprot (downloaded January 12, 2021) and quantify protein expression by label-free quantitation (LFQ). MaxQuant results were

processed using both LFQ analyst[25] and Perseus (v1.6.14.0).[26] To allow for statistical analysis of the data, data imputation was carried out in Perseus (for Perseus-type imputation, missing values are replaced by random numbers drawn from a normal distribution with a width of 0.3 and down shift of 1.8).[26] Significance testing in Perseus was performed using a two-tailed Student's *t*-test with P-value truncation and threshold P-value of 0.05. Protein network analysis of differentially expressed proteins was performed using STRING 11.0[27] and Cytoscape 3.8.2.[28] Gene ontology (GO) analysis was performed in STRING, using the 22,763 distinct protein encoding genes in the *Rattus norvegicus* database as the enrichment background.

Results and discussion

Rbm20 KO rats

To identify changes in the rat cardiac proteome associated with Rbm20 KO, we carried out proteomic analysis of hearts from 3-week-old Rbm20 KO rats. The Rbm20 KO rat strain contains a spontaneous deletion of ~95-kb on the long arm of chromosome 1 that removes all exons following exon 1 of the *Rbm20* gene.[11] Consequently, these rats do not express Rbm20 at either the transcript or protein levels.[11] Our previous analysis of cardiac function in these rats revealed that they develop DCM with chamber dilation and cardiac dysfunction by 6-months-of-age.[29] However, rats up to 3-months-of-age lack any apparent phenotype with cardiac structure and function being similar to that in age-matched WT rats despite decreased myocardial stiffness resulting from titin isoform switching.[29] To identify changes in the cardiac proteome associated with Rbm20 ablation, we chose to study rats at 3-weeks-of-age (21 days) as interrogation of the cardiac proteome at this timepoint would be expected to provide insights into proteome changes associated with Rbm20 loss while avoiding confounding changes associated with DCM itself.

Reproducibility of protein extraction and LC-MS analysis

To assess changes in the cardiac proteome associated with Rbm20 deficiency, proteins were extracted from the myocardium of 3-week-old WT and KO rats (n = 8 each) using a one-step protein extraction procedure with the photocleavable MS-compatible surfactant Azo (Fig. 1A).[21] Analysis of protein extracts by SDS-PAGE with Coomassie blue staining confirmed highly reproducible protein extraction from both WT and KO rat myocardium across biological replicates (Fig. 1B).

Consistent with the reproducibility of protein extraction, LC-MS/MS analysis of protein extracts yielded total ion chromatograms that were consistent across WT and KO biological replicates (Fig. S1). Moreover, $\log_2$ transformed peptide intensities were in accordance across biological replicates as indicated by average Pearson correlation coefficients of 0.98 and 0.97 for all WT and KO biological replicates, respectively (Fig. 1C). To determine whether the protein intensity profiles were similar across WT and KO biological replicates, individual $\log_2$ transformed peptide LFQ intensities were binned and plotted in histograms. As shown in Fig. S2 and S3, protein intensity profiles were in good agreement across WT and KO biological replicates, respectively. Collectively, these results demonstrate the high reproducibility of protein extraction and LC-MS analysis.

Identification of proteins in myocardial extracts prepared from WT and KO rats

A total of 2,425 and 2,379 proteins were identified by LC-MS/MS in all WT and KO biological replicates, respectively (Table S1, S2). It should be noted that these numbers are lower than the number of identifications previously obtained from human myocardial protein extracts (approximately 4,000 protein identifications) using the same method.[21] This difference can be explained by the fact that the rat database lacks the completeness of the human database, with only one fifth the number of human entries. Comparison of the protein identifications between WT and KO rat samples yielded a list of 2,287 proteins that could be reproducibly quantified across all 16 samples, with an additional 138 and 91 unique proteins that could only be quantified in WT and KO ventricular myocardium, respectively (Fig. 2A). To assess patterns among WT and KO biological replicates principal component analysis (PCA) was performed. As expected, PCA showed that biological replicates were generally clustered into two groups, one containing the biological replicates from WT and the other KO biological replicates (Fig. 2B)—a result that highlights the difference between the WT and KO cardiac proteomes.

Differentially expressed proteins (DEPs) in Rbm20 KO rat myocardium contribute to pathological cardiac remodeling

Quantitative global proteomic analysis enabled the identification of 103 proteins that are differentially expressed in KO versus WT rat myocardium (Fig. 3). Of the 103 DEPs, 48 and 55 were up- and down-regulated, respectively, in KO relative to WT. Differences in the expression levels of the nine proteins with the highest $-\log_{10}$ p-values are shown in boxplots to visualize the spread in protein LFQ values for individual biological replicates (Fig. S4). Not surprisingly, one of the proteins with the greatest change in expression was Rbm20 (Fig. 3, S4), which was not detected in any of the KO rat samples consistent with the complete loss of Rbm20 transcript and protein expression in this rat model.[11] Note that the values for Rbm20 shown in Fig. S4 for the KO rat samples are the result of data imputation to replace the missing values and allow for statistical analysis in the Perseus software platform (see Methods). As expected, comparison of the list of DEPs to previously identified differentially expressed genes revealed several discrepancies between the proteomics and transcriptomics data at 20 days post-birth, although several changes were consistent, such as upregulation of proenkephalin-A (Penk) (Table S3). Additionally, to identify common processes and functions, as well as interactions, among the DEPs, the gene ontology (GO) and STRING databases were searched using the list of DEPs (Figs. 4–5, S5).

Notably, quantitative proteomics analysis identified changes in the expression of several titin-interacting proteins in KO rat myocardium. We have previously shown that four and a half LIM domains 1 (Fhl1) and ankyrin repeat domain 1 (Ankrd1, also known as cardiac ankyrin repeat protein or Carp) are upregulated at the transcript level in KO rat myocardium.[12] Upregulated expression of Fhl1 in the Rbm20 KO rat ventricle has also been confirmed at the protein level previously using Western blot.[12] Herein, quantitative proteomic analysis allowed us to confirm the upregulation of *Ankrd1* at the protein level at 21 days after birth even though protein transcript expression was not changed until 49 days post-birth for Ankrd1 (Table S3),[12] and also identify a decrease in the expression of four and a half LIM domains 2 (Fhl2) (Fig. 3). Ankrd1 has been shown to bind to the N2A region of

titin,[30] and is a functionally pleiotropic protein that plays roles in transcriptional regulation, sarcomere assembly, and mechano-transduction in the heart.[31] Importantly, Ankrd1 is upregulated in response to hypertrophic stimuli and in human heart failure;[32,33] and plays a direct role in hypertrophic gene expression via modulation of Erk/Gata4 phosphorylation.[34] Fhl1 has previously been shown to exist as part of a biomechanical stretch sensor complex that is localized to the titin N2B spring element and, similar to Ankrd1, has been shown to be important for the development of stress-induced pathological cardiac hypertrophy.[35] STRING network analysis showed an interaction between Ankrd1 and Fhl2 (Fig. 5), and indeed there is evidence in the literature supporting a direct interaction between Ankrd1 and Fhl2.[36] However, in contrast to Ankrd1, previous studies have demonstrated that Fhl2 negatively regulates cardiac hypertrophy.[37] Specifically, prior studies have shown that Fhl2 prevents activation of the hypertrophic transcription factor NFAT through interactions with activated calcineurin—the phosphatase responsible for dephosphorylating and, thus, activating NFAT.[37] Collectively, these changes suggest that alterations in titin-interacting proteins involved in mechanical stretch-based signaling and hypertrophic gene program induction in Rbm20 KO rats may contribute to the development of pathological cardiac remodeling in KO animals.

Pathological phenotype in Rbm20 KO rats is associated with altered mitochondrial metabolism and/or dysfunction

Gene ontology (GO) analysis revealed that many of the DEPs are involved in metabolism, including organic substance metabolism, cellular metabolism, and metabolic processes (Fig. 4). In agreement with this, the most highly downregulated protein in the KO rat myocardium was 3-hydroxy-3-methylglutaryl-CoA synthase 2 (Hmgcs2), a key mitochondrial enzyme that catalyzes the rate-limiting step in ketogenesis.[38] Notably, we previously found that Hmgcs2 is downregulated at the transcript level for at least 20 days following birth in Rbm20 KO rat myocardium, although expression was not significantly different between WT and KO at 49 days post-birth (Table S4).[12] In addition, the expression of several other proteins with the GO designation “mitochondrion” (GO: 0005739), including enoyl-CoA hydratase 1 (Ech1), pyruvate dehydrogenase kinase 4 (Pdk4), and aldehyde dehydrogenase 1 family member B1 (Aldh1b1), was downregulated in KO rat myocardium (Fig. 3). Our previous analysis uncovered several other differentially expressed genes at the transcript level, including Ccnb1, Dguok, and Trub1, all of which were upregulated 20 days after birth (Table S4).[12]

In addition to these changes, the mitochondrial chaperone TNF receptor associated protein 1 (Trap1), a member of the HSP90 protein family, was also significantly upregulated in KO versus WT rat myocardium (Fig. 3). A prior study has shown that Trap1 expression protects against myocardial ischemia/reperfusion injury by limiting mitochondrial dysfunction.[39] Moreover, the protein with the greatest increase in expression in the KO rat myocardium was mitochondrial methionine-R-sulfoxide reductase B2 (Msrb2) (Fig. 3A), which has previously been implicated in mitophagy,[40] a cellular process that removes damaged or unneeded mitochondria.[41] Increased expression of Msrb2 in the Rbm20 KO rat myocardium was confirmed by Western blot (Fig. 3B-C). Our group and others have previously shown that the intracellular calcium concentration is increased during diastole in cardiomyocytes

from Rbm20 KO rats and mice relative to that in cells from WT rats and mice.[12,13] Given the exquisite sensitivity of mitochondria to intracellular calcium concentrations,[42] it is tempting to speculate that increased Msrb2 may reflect an upregulation of mitophagy to remove damaged/dysfunctional mitochondria and limit cardiomyocyte cell death resulting from mitochondrial calcium overload in Rbm20 KO rats. Nevertheless, it is worth noting that not all identified mitochondrial proteins were downregulated in the hearts of Rbm20 KO rats. Thus, whether the observed changes are reflective of mitochondrial removal or broad rewiring of mitochondrial metabolism will require further investigation. Nevertheless, taken together these findings implicate altered cellular metabolism in the development of DCM secondary to Rbm20 loss.

Conclusion

In summary, herein we employed global quantitative MS-based proteomics to identify changes in the cardiac proteome in Rbm20 KO rats and gain insight into alterations potentially involved in the development of DCM resulting from Rbm20 ablation. Our proteomics analysis uncovered changes in the expression of several known titin-interacting proteins congruent with the induction of pathological cardiac hypertrophy. In addition, we found that the expression of a number of metabolic enzymes localizing to the mitochondria was decreased concomitant with the upregulation of the mitochondrial chaperone Trap1 in Rbm20 KO rat myocardium. These changes are consistent with the idea that Rbm20 ablation is associated with altered mitochondrial metabolism and dysfunction, which may contribute to the development of DCM. Moreover, the upregulation of Msrb2—a protein previously implicated in mitophagy—in the myocardium of Rbm20 KO rats is consistent with this notion and may be an adaptive change to clear dysfunctional mitochondria from cardiomyocytes. It should be noted that, although studying changes in the cardiac proteome of Rbm20 KO rats at 3-weeks-of-age avoids confounding changes associated with DCM, myocardial stiffness is altered in these mice due to titin isoform switching and could contribute to the detected changes in protein expression. Moreover, as Rbm20 is a splicing factor, changes in the splicing of Rbm20 target transcripts likely play an important role in DCM development in Rbm20 KO rats, however, changes in splice isoform expression are difficult to quantify using peptide-based proteomics approaches such as that employed in this study as peptide recovery is limited and recovered peptides often map to multiple protein isoforms (the so called “protein inference problem”[43]). Nevertheless, these findings provide the first report on changes in the cardiac proteome associated with loss of Rbm20 and highlight several changes in the cardiac proteome of Rbm20 KO rats that may contribute to the development of DCM independent of alterations in splicing.

Supplementary Material

Refer to Web version on PubMed Central for supplementary material.

Acknowledgements

This research was supported by funding from NHLBI (HL148733), NICHD (HD101870), and the AHA (19TPA34830072) (to W.G.). Y.G. would like to acknowledge NIH R01 HL096971, R01 HL109810, and S10 OD018475.

References

1. Schultheiss HP, Fairweather D, Caforio ALP, Escher F, Hershberger RE, Lipshultz SE, Liu PP, Matsumori A, Mazzanti A, McMurray J, et al. Dilated cardiomyopathy. Nat Rev Dis Primers. 2019;5:32. doi: 10.1038/s41572-019-0084-1 [PubMed: 31073128]
2. Hershberger RE, Hedges DJ, Morales A. Dilated cardiomyopathy: the complexity of a diverse genetic architecture. Nat Rev Cardiol. 2013;10:531–547. doi: 10.1038/nrcardio.2013.105 [PubMed: 23900355]
3. Herman DS, Lam L, Taylor MR, Wang L, Teekakirikul P, Christodoulou D, Conner L, DePalma SR, McDonough B, Sparks E, et al. Truncations of titin causing dilated cardiomyopathy. N Engl J Med. 2012;366:619–628. doi: 10.1056/NEJMoa1110186 [PubMed: 22335739]
4. Pérez-Serra A, Toro R, Sarquella-Brugada G, de Gonzalo-Calvo D, Cesar S, Carro E, Llorente-Cortes V, Iglesias A, Brugada J, Brugada R, et al. Genetic basis of dilated cardiomyopathy. Int J Cardiol. 2016;224:461–472. doi: 10.1016/j.ijcard.2016.09.068 [PubMed: 27736720]
5. Wang C, Zhang Y, Methawasin M, Braz CU, Gao-Hu J, Yang B, Strom J, Gohlke J, Hacker T, Khatib H, et al. RBM20. J Mol Cell Cardiol. 2022;165:115–129. doi: 10.1016/j.yjmcc.2022.01.004 [PubMed: 35041844]
6. Schneider JW, Oommen S, Qureshi MY, Goetsch SC, Pease DR, Sundsbak RS, Guo W, Sun M, Sun H, Kuroyanagi H, et al. Dysregulated ribonucleoprotein granules promote cardiomyopathy in RBM20 gene-edited pigs. Nat Med. 2020;26:1788–1800. doi: 10.1038/s41591-020-1087-x [PubMed: 33188278]
7. Ihara K, Sasano T, Hiraoka Y, Togo-Ohno M, Soejima Y, Sawabe M, Tsuchiya M, Ogawa H, Furukawa T, Kuroyanagi H. A missense mutation in the RSRSP stretch of Rbm20 causes dilated cardiomyopathy and atrial fibrillation in mice. Sci Rep. 2020;10:17894. doi: 10.1038/s41598-020-74800-8 [PubMed: 33110103]
8. Zhang Y, Wang C, Sun M, Jin Y, Braz CU, Khatib H, Hacker TA, Liss M, Gotthardt M, Granzier H, et al. RBM20 phosphorylation and its role in nucleocytoplasmic transport and cardiac pathogenesis. FASEB J. 2022;36:e22302. doi: 10.1096/fj.202101811RR [PubMed: 35394688]
9. Haas J, Frese KS, Peil B, Kloos W, Keller A, Nietsch R, Feng Z, Müller S, Kayvanpour E, Vogel B, et al. Atlas of the clinical genetics of human dilated cardiomyopathy. Eur Heart J. 2015;36:1123–1135a. doi: 10.1093/eurheartj/ehu301 [PubMed: 25163546]
10. Kayvanpour E, Sedaghat-Hamedani F, Gi WT, Tugrul OF, Amr A, Haas J, Zhu F, Ehlermann P, Uhlmann L, Katus HA, et al. Clinical and genetic insights into non-compaction: a meta-analysis and systematic review on 7598 individuals. Clin Res Cardiol. 2019;108:1297–1308. doi: 10.1007/s00392-019-01465-3 [PubMed: 30980206]
11. Guo W, Schafer S, Greaser ML, Radke MH, Liss M, Govindarajan T, Maatz H, Schulz H, Li S, Parrish AM, et al. RBM20, a gene for hereditary cardiomyopathy, regulates titin splicing. Nat Med. 2012;18:766–773. doi: 10.1038/nm.2693 [PubMed: 22466703]
12. Guo W, Zhu C, Yin Z, Wang Q, Sun M, Cao H, Greaser ML. Splicing Factor RBM20 Regulates Transcriptional Network of Titin Associated and Calcium Handling Genes in The Heart. Int J Biol Sci. 2018;14:369–380. doi: 10.7150/ijbs.24117 [PubMed: 29725258]
13. van den Hoogenhof MMG, Beqqali A, Amin AS, van der Made I, Aufiero S, Khan MAF, Schumacher CA, Jansweijer JA, van Spaendonck-Zwarts KY, Remme CA, et al. RBM20 Mutations Induce an Arrhythmogenic Dilated Cardiomyopathy Related to Disturbed Calcium Handling. Circulation. 2018;138:1330–1342. doi: 10.1161/CIRCULATIONAHA.117.031947 [PubMed: 29650543]
14. Methawasin M, Hutchinson KR, Lee EJ, Smith JE, Saripalli C, Hidalgo CG, Ottenheijm CA, Granzier H. Experimentally increasing titin compliance in a novel mouse model attenuates the Frank-Starling mechanism but has a beneficial effect on diastole. Circulation. 2014;129:1924–1936. doi: 10.1161/CIRCULATIONAHA.113.005610 [PubMed: 24599837]
15. de Sousa Abreu R, Penalva LO, Marcotte EM, Vogel C. Global signatures of protein and mRNA expression levels. Mol Biosyst. 2009;5:1512–1526. doi: 10.1039/b908315d [PubMed: 20023718]

16. Vogel C, Marcotte EM. Insights into the regulation of protein abundance from proteomic and transcriptomic analyses. Nat Rev Genet. 2012;13:227–232. doi: 10.1038/nrg3185 [PubMed: 22411467]

17. Maier T, Güell M, Serrano L. Correlation of mRNA and protein in complex biological samples. FEBS Lett. 2009;583:3966–3973. doi: 10.1016/j.febslet.2009.10.036 [PubMed: 19850042]

18. Brown KA, Chen B, Guardado-Alvarez TM, Lin Z, Hwang L, Ayaz-Guner S, Jin S, Ge Y. A photocleavable surfactant for top-down proteomics. Nat Methods. 2019;16:417–420. doi: 10.1038/s41592-019-0391-1 [PubMed: 30988469]

19. Brown KA, Tucholski T, Eken C, Knott S, Zhu Y, Jin S, Ge Y. High-Throughput Proteomics Enabled by a Photocleavable Surfactant. Angew Chem Int Ed Engl. 2020;59:8406–8410. doi: 10.1002/anie.201915374 [PubMed: 32097521]

20. Guo W, Pleitner JM, Saupe KW, Greaser ML. Pathophysiological defects and transcriptional profiling in the RBM20−/− rat model. PLoS One. 2013;8:e84281. doi: 10.1371/journal.pone.0084281 [PubMed: 24367651]

21. Aballo TJ, Roberts DS, Melby JA, Buck KM, Brown KA, Ge Y. Ultrafast and Reproducible Proteomics from Small Amounts of Heart Tissue Enabled by Azo and timsTOF Pro. J Proteome Res. 2021;20:4203–4211. doi: 10.1021/acs.jproteome.1c00446 [PubMed: 34236868]

22. Jin Y, Wei L, Cai W, Lin Z, Wu Z, Peng Y, Kohmoto T, Moss RL, Ge Y. Complete Characterization of Cardiac Myosin Heavy Chain (223 kDa) Enabled by Size-Exclusion Chromatography and Middle-Down Mass Spectrometry. Anal Chem. 2017;89:4922–4930. doi: 10.1021/acs.analchem.7b00113 [PubMed: 28366003]

23. Meier F, Brunner AD, Koch S, Koch H, Lubeck M, Krause M, Goedecke N, Decker J, Kosinski T, Park MA, et al. Online Parallel Accumulation-Serial Fragmentation (PASEF) with a Novel Trapped Ion Mobility Mass Spectrometer. Mol Cell Proteomics. 2018;17:2534–2545. doi: 10.1074/mcp.TIR118.000900 [PubMed: 30385480]

24. Schneider CA, Rasband WS, Eliceiri KW. NIH Image to ImageJ: 25 years of image analysis. Nat Methods. 2012;9:671–675. [PubMed: 22930834]

25. Shah AD, Goode RJA, Huang C, Powell DR, Schittenhelm RB. LFQ-Analyst: An Easy-To-Use Interactive Web Platform To Analyze and Visualize Label-Free Proteomics Data Preprocessed with MaxQuant. J Proteome Res. 2020;19:204–211. doi: 10.1021/acs.jproteome.9b00496 [PubMed: 31657565]

26. Tyanova S, Temu T, Sinitcyn P, Carlson A, Hein MY, Geiger T, Mann M, Cox J. The Perseus computational platform for comprehensive analysis of (prote)omics data. Nat Methods. 2016;13:731–740. doi: 10.1038/nmeth.3901 [PubMed: 27348712]

27. Szklarczyk D, Gable AL, Nastou KC, Lyon D, Kirsch R, Pyysalo S, Doncheva NT, Legeay M, Fang T, Bork P, et al. The STRING database in 2021: customizable protein-protein networks, and functional characterization of user-uploaded gene/measurement sets. Nucleic Acids Res. 2021;49:D605–D612. doi: 10.1093/nar/gkaa1074 [PubMed: 33237311]

28. Shannon P, Markiel A, Ozier O, Baliga NS, Wang JT, Ramage D, Amin N, Schwikowski B, Ideker T. Cytoscape: a software environment for integrated models of biomolecular interaction networks. Genome Res. 2003;13:2498–2504. doi: 10.1101/gr.1239303 [PubMed: 14597658]

29. Guo W, Zhu C, Yin Z, Zhang Y, Wang C, Walk AS, Lin YH, McKinsey TA, Woulfe KC, Ren J, et al. The ryanodine receptor stabilizer S107 ameliorates contractility of adult Rbm20 knockout rat cardiomyocytes. Physiol Rep. 2021;9:e15011. doi: 10.14814/phy2.15011 [PubMed: 34523260]

30. Miller MK, Bang ML, Witt CC, Labeit D, Trombitas C, Watanabe K, Granzier H, McElhinny AS, Gregorio CC, Labeit S. The muscle ankyrin repeat proteins: CARP, ankrd2/Arpp and DARP as a family of titin filament-based stress response molecules. J Mol Biol. 2003;333:951–964. doi: 10.1016/j.jmb.2003.09.012 [PubMed: 14583192]

31. Ling SSM, Chen YT, Wang J, Richards AM, Liew OW. Ankyrin Repeat Domain 1 Protein: A Functionally Pleiotropic Protein with Cardiac Biomarker Potential. Int J Mol Sci. 2017;18. doi: 10.3390/ijms18071362 [PubMed: 29267212]

32. Aihara Y, Kurabayashi M, Saito Y, Ohyama Y, Tanaka T, Takeda S, Tomaru K, Sekiguchi K, Arai M, Nakamura T, et al. Cardiac ankyrin repeat protein is a novel marker of cardiac

hypertrophy: role of M-CAT element within the promoter. Hypertension. 2000;36:48–53. doi: 10.1161/01.hyp.36.1.48 [PubMed: 10904011]

33. Zolk O, Frohme M, Maurer A, Kluxen FW, Hentsch B, Zubakov D, Hoheisel JD, Zucker IH, Pepe S, Eschenhagen T. Cardiac ankyrin repeat protein, a negative regulator of cardiac gene expression, is augmented in human heart failure. Biochem Biophys Res Commun. 2002;293:1377–1382. doi: 10.1016/S0006-291X(02)00387-X [PubMed: 12054667]
34. Jing J, He L, Sun A, Quintana A, Ding Y, Ma G, Tan P, Liang X, Zheng X, Chen L, et al. Proteomic mapping of ER-PM junctions identifies STIMATE as a regulator of Ca^{2+} influx. Nat Cell Biol. 2015;17:1339–1347. doi: 10.1038/ncb3234 [PubMed: 26322679]
35. Sheikh F, Raskin A, Chu PH, Lange S, Domenighetti AA, Zheng M, Liang X, Zhang T, Yajima T, Gu Y, et al. An FHL1-containing complex within the cardiomyocyte sarcomere mediates hypertrophic biomechanical stress responses in mice. J Clin Invest. 2008;118:3870–3880. doi: 10.1172/JCI34472 [PubMed: 19033658]
36. Zhong L, Chiusa M, Cadar AG, Lin A, Samaras S, Davidson JM, Lim CC. Targeted inhibition of ANKRD1 disrupts sarcomeric ERK-GATA4 signal transduction and abrogates phenylephrine-induced cardiomyocyte hypertrophy. Cardiovasc Res. 2015;106:261–271. doi: 10.1093/cvr/cvv108 [PubMed: 25770146]
37. Hojayev B, Rothermel BA, Gillette TG, Hill JA. FHL2 binds calcineurin and represses pathological cardiac growth. Mol Cell Biol. 2012;32:4025–4034. doi: 10.1128/MCB.05948-11 [PubMed: 22851699]
38. Vilà-Brau A, De Sousa-Coelho AL, Mayordomo C, Haro D, Marrero PF. Human HMGCS2 regulates mitochondrial fatty acid oxidation and FGF21 expression in HepG2 cell line. J Biol Chem. 2011;286:20423–20430. doi: 10.1074/jbc.M111.235044 [PubMed: 21502324]
39. Zhang P, Lu Y, Yu D, Zhang D, Hu W. TRAP1 Provides Protection Against Myocardial Ischemia-Reperfusion Injury by Ameliorating Mitochondrial Dysfunction. Cell Physiol Biochem. 2015;36:2072–2082. doi: 10.1159/000430174 [PubMed: 26202366]
40. Lee SH, Lee S, Du J, Jain K, Ding M, Kadado AJ, Atteya G, Jaji Z, Tyagi T, Kim WH, et al. Mitochondrial MsrB2 serves as a switch and transducer for mitophagy. EMBO Mol Med. 2019;11:e10409. doi: 10.15252/emmm.201910409 [PubMed: 31282614]
41. Palikaras K, Lionaki E, Tavernarakis N. Mechanisms of mitophagy in cellular homeostasis, physiology and pathology. Nat Cell Biol. 2018;20:1013–1022. doi: 10.1038/s41556-018-0176-2 [PubMed: 30154567]
42. Ramaccini D, Montoya-Uribe V, Aan FJ, Modesti L, Potes Y, Wieckowski MR, Krga I, Glibetić M, Pinton P, Giorgi C, et al. Mitochondrial Function and Dysfunction in Dilated Cardiomyopathy. Front Cell Dev Biol. 2020;8:624216. doi: 10.3389/fcell.2020.624216 [PubMed: 33511136]
43. Nesvizhskii AI, Aebersold R. Interpretation of shotgun proteomic data: the protein inference problem. Mol Cell Proteomics. 2005;4:1419–1440. doi: 10.1074/mcp.R500012-MCP200 [PubMed: 16009968]

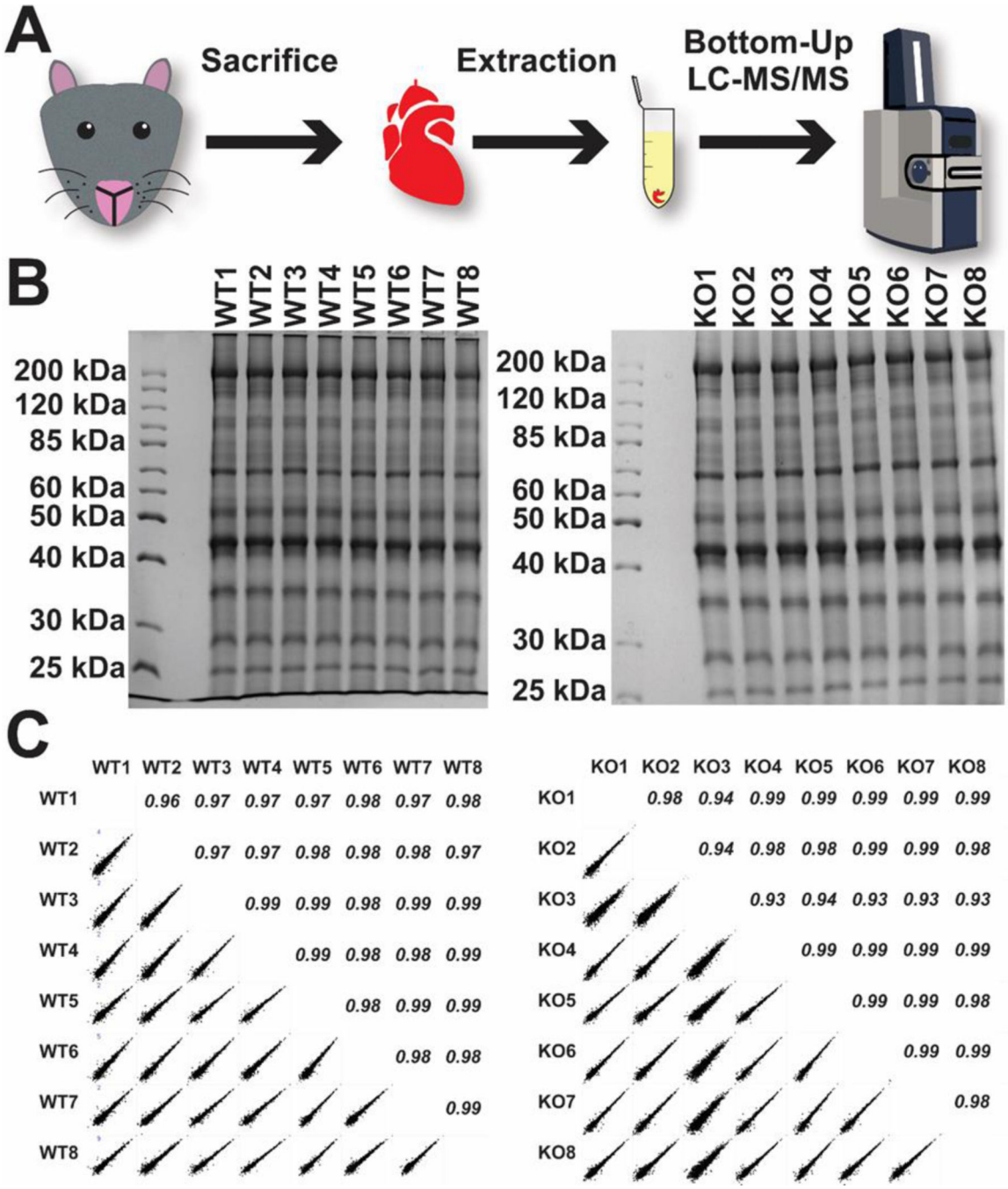

Figure 1.

Schematic showing the experimental workflow with protein extraction and LC-MS/MS analysis (A). Using a one-step Azo-enabled extraction, ventricular tissue from WT and Rbm20 KO rats (n = 8 each) was analyzed. SDS-PAGE confirmed reproducibility of extraction performance for both WT and KO replicates (B). Pearson correlation analysis was performed among biological replicates and average Pearson's correlation coefficients of 0.98 and 0.97 were obtained for WT and KO replicates, respectively (C).

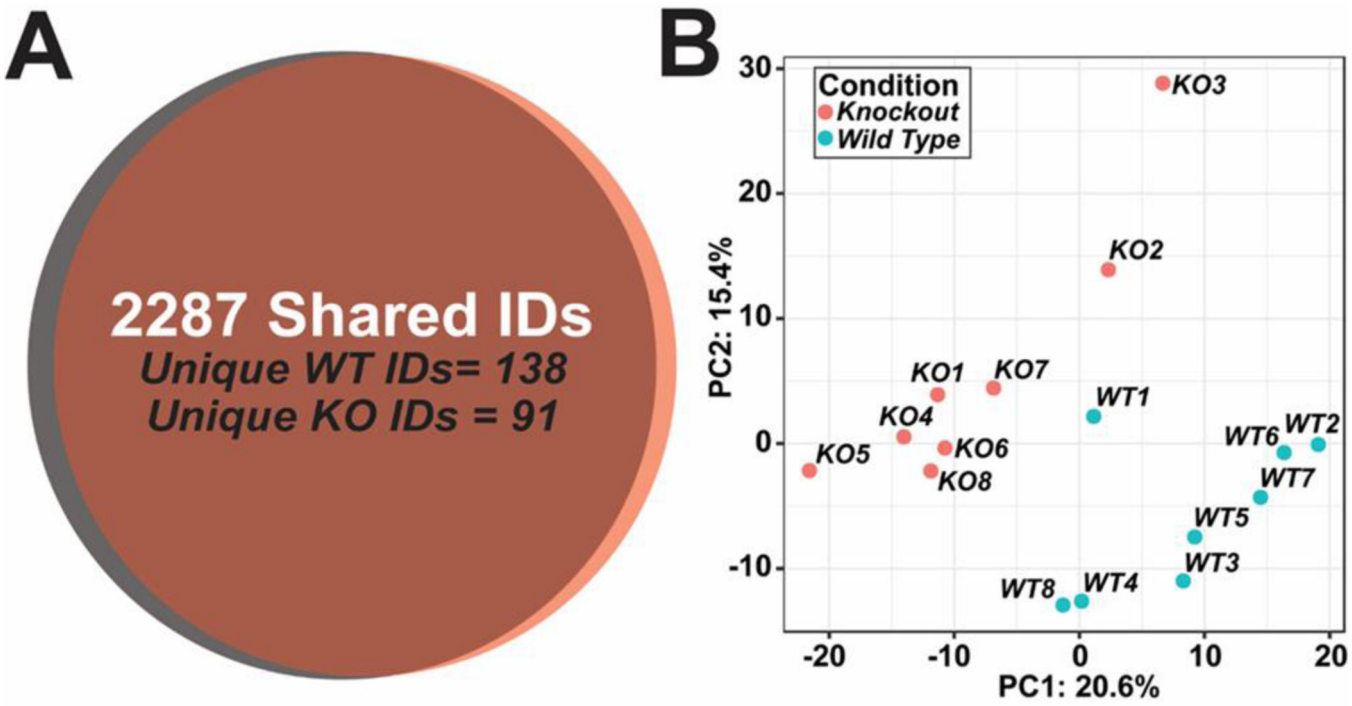

Figure 2.

Bottom-up LC-MS/MS analysis with the timsTOF Pro identified 2,287 proteins common to all WT and KO samples, with 138 additional proteins unique to the eight WT rats and 91 proteins unique to the eight Rbm20 KO rats (A). Principal component analysis was performed for all WT and Rbm20 KO biological replicates (B).

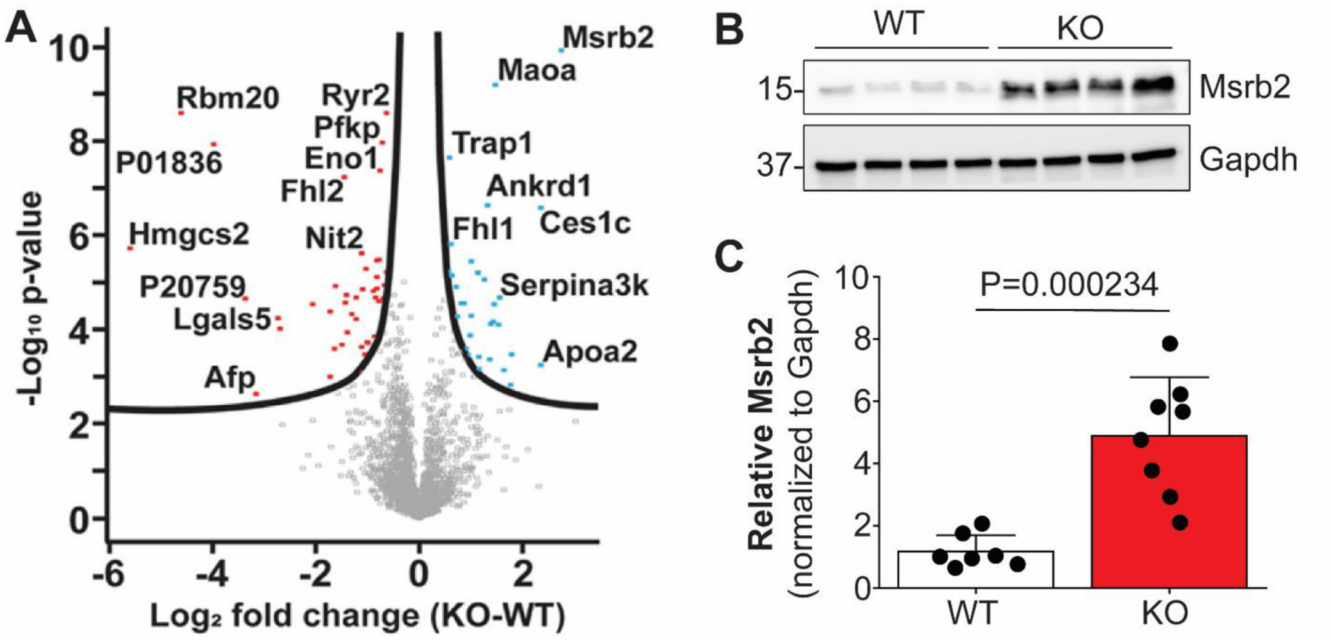

Figure 3.

Volcano plot showing the 103 proteins that are differentially expressed in Rbm20 KO versus WT rat myocardium (A). Western blot analysis of Msrb2 expression in Rbm20 WT (n=7) and KO (n=8) rat myocardium. B. Representative Western blot showing Msrb2 expression in Rbm20 WT and KO rat ventricular myocardium. Gapdh served as a loading control. C. Quantification of Msrb2 expression. Bar graphs indicate mean ± SD. The significance of the difference between group means was determined using a two-tailed Student's *t*-test.

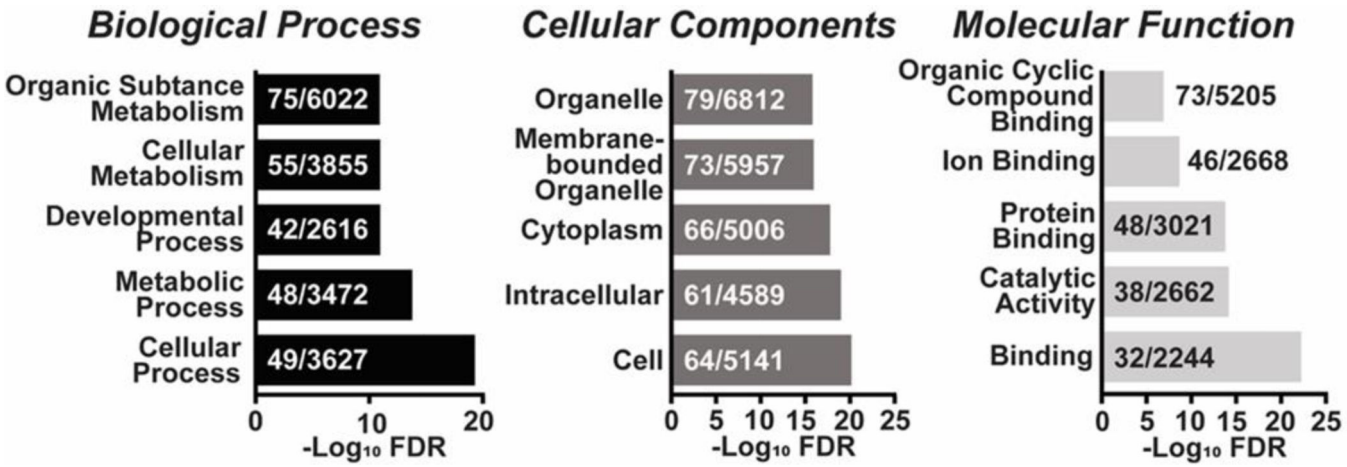

Figure 4.

GO analysis using STRING for the top-5 terms is plotted against the $-\text{Log}_{10}$ FDR, with the number of identified proteins associated with the specific GO term versus the total number of identified proteins overlaid on the bar chart bars.

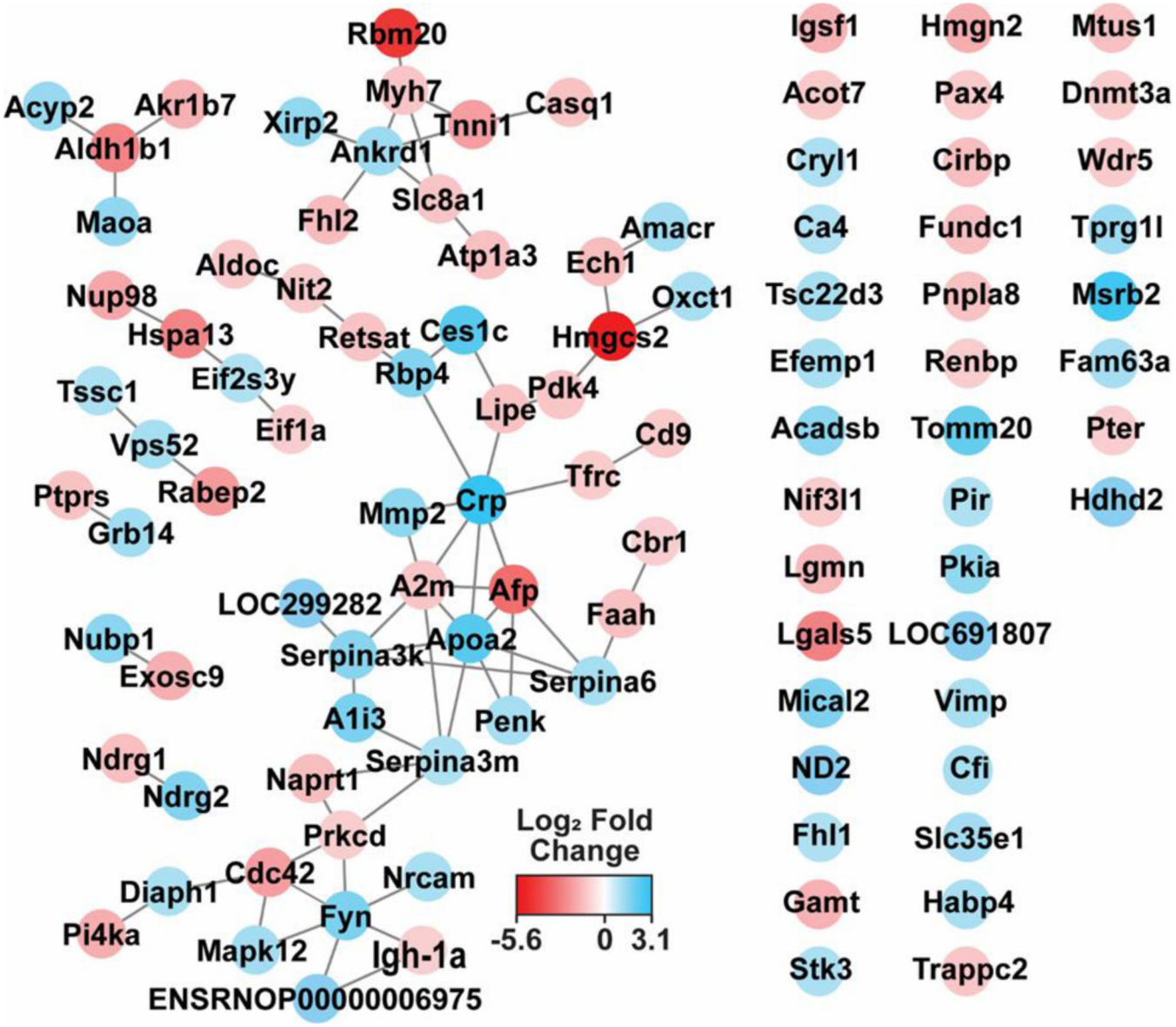

Figure 5.

String-generated interaction map for known proteins, with nodes colored by Log2 fold change in expression. Based on information from the String database, 62 DEPs had known interactors amongst the 103 differentially expressed proteins, while 38 had no known interactors.